Channel Capacity of MIMO Wideband CDMA System under the Imperfect Channel Estimation and Near/Far Effect

Jae-Sung Roh[1], Hyung-Rae Park[2], and Sung-Joon Cho[2]

1 Dept. of Information & Communication Eng.,
SEOIL College, Seoul, Korea
jsroh@seoil.ac.kr
2 School of Electronics, Telecommunication and Computer Eng.,
Hankuk Aviation Univ.,
Kyonggi-do, Korea
{hrpark,sjcho}@mail.hangkong.ac.kr

Abstract. The channel capacity of multiple-input multiple-output (MIMO) wideband CDMA system with coherent RAKE receiver is considered. General multi-path intensity Nakagami fading and multiple-access near/far interference channel are assumed. The analysis for system performance shows that the error of channel estimation significantly degrades BER performance and can be effectively suppressed by RAKE receiver and MIMO schemes. Also, an attempt for comparing the channel capacity on different performance improvement schemes has been made. In particular, the channel capacity of MIMO system is compared with single-input single-output (SISO) system. The MIMO complex spreading CDMA system with path correlation yields better performance with respect to channel capacity than a SISO system with i.i.d. input and output. And a discussion on the multiple-access near/far interference is also included, which illustrates that it can be effectively limited by power control and channel estimation schemes.

1 Introduction

To provide higher data rates for end users, as well as to accommodate more users over wireless channels in the next generation communication systems, wideband CDMA has become the focus of current research interests. Two of the important features of wideband CDMA systems are the use of complex spreading and user-dedicated pilot channel [1]-[5]. Coherent reception requires the knowledge of channel characteristics, which are time varying in fading environments [6]. A conventional and effective method to accomplish this task is to use a separate pilot channel or insert pilot symbols in data symbols.

Generally, multi-path is viewed as an undesirable feature of wireless communications. Recently, to increase the spectrum efficiency and the link reliability, multiple-input multiple-output (MIMO) scheme is devised to exploit multi-path in a scattering wireless channel. Previous results about MIMO channel [7], [8] confirm that the enormous capacity gain is obtained by using the multi-element antennas. In

M. Conti et al. (Eds.): PWC 2003, LNCS 2775, pp. 407–416, 2003.

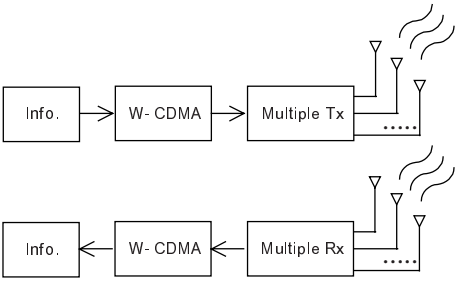

Fig. 1. System structure of MIMO W-CDMA.

order to improve the channel capacity, the signals at various elements must be uncorrelated. But multi-path components arrive from a wide range of azimuth angles in a heavy scattering channel. If the paths are correlated due to inappropriate spacing or mutual coupling effects, the channel capacity becomes substantially smaller.

In this paper, the channel capacity of MIMO wideband CDMA system with imperfect channel estimation and multiple-access near/far interference is evaluated. The channel capacity improvement due to the RAKE receiving and multiple antenna schemes is also investigated in order to achieve reliable performance of wideband CDMA system.

2 System Model

The system structure of MIMO wideband CDMA system is shown in Fig. 1, where *M* transmitting antennas send the wideband CDMA signal over scattering wireless channel to *M* receiving antennas at each symbol time.

2.1 Transmitter Model

In the reverse link of wideband CDMA systems, where an I/Q code-multiplexed pilot is utilized, spreading consists of two operations. The first is channelization operation, in which pilot and data symbols on I- and Q-branches are independently multiplied with an orthogonal variable spreading factor code and transformed into a number of chips. The second operation is scrambling, where the resultant signal are further multiplied by a complex valued scrambling code. This spreading scheme is called complex spreading, as illustrated in figure 2(a).

The transmitted signal of the *k*-th user can be written as [1]

$$
\begin{aligned}
S_j(t) = \sqrt{E_{D,j}} \sum_{n=-\infty}^{\infty} \{ & \\
& \cdot \left[\sqrt{g_j} C_{P,j}(n) S_I(n) - D_j(m) C_{D,j}(n) S_Q(n) \right] \\
& \cdot h(t - nT_c) \cos(\omega_o t + \phi_j) \\
& \cdot - \left[\sqrt{g_j} C_{P,j}(n) S_Q(n) - D_j(m) C_{D,j}(n) S_I(n) \right] \\
& \cdot h(t - nT_c) \sin(\omega_o t + \phi_j) \quad \}
\end{aligned}
\tag{1}
$$

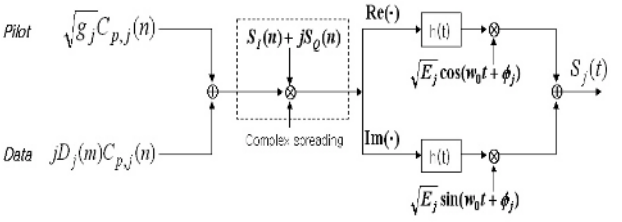

(a) Transmitter model

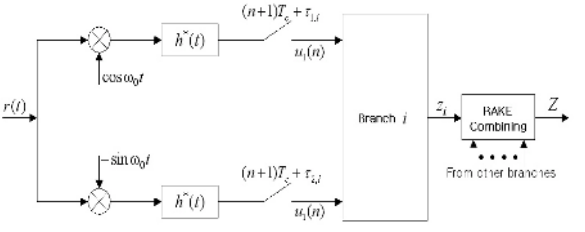

(b) Receiver model

Fig. 2. Transmitter and RAKE receiver model of the k-user.

where $E_{D,j}$ is chip energy of data channel, g_j is power ratio of pilot channel to the data channel, $D_j(m)$ is data symbols for the *j*-th user, ϕ_j is carrier phase, $C_{P,j}(n)$ and $C_{D,j}(n)$ are orthogonal channel codes for pilot and data symbols, respectively, $S_I(n)$ and $S_Q(n)$ are real and imaginary parts, respectively, of the cell-specific scrambling sequence, $h(t)$ is impulse response of the pulse shaping filter truncated by the length of AT_c for practical systems, where $A>1$, and T_c is the chip interval. And, the power of the transmitted signal is expressed as

$$P_j = (1+g_j)\,E_{D,j}/T_c = E_j/T_c \tag{2}$$

where E_j is the chip energy for both data channel and dedicate pilot channel of the *j*-th user.

2.2 Channel and Receiver Model

The complex low-pass equivalent impulse response of a multi-path fading channel can be written as

$$h_j(t) = \sum_{l=0}^{L-1} \alpha_{j,l}(t)\,\delta[t-\tau_{j,l}(t)]\,e^{j\theta_{j,l}(t)} \tag{3}$$

where L ($L \geq 1$) is the number of resolvable propagation paths. For the sake of simple notation, it is assumed that all users have the same number of multi-paths. $\alpha_{j,l}(t)e^{j\theta_{j,l}(t)}$

and $\tau_{j,l}(t)$ are the complex fading factor and propagation delay of the *l*-th path of the *j*-th user, respectively, and $\alpha_{j,l}(t)$ is frequency selective Nakagami-distributed in MIMO channel model. All random variables in (3) are assumed independent for *j* and *l*. The amplitude fading in each path is assumed to be Nakagami distributed since the Nakagami distribution is more versatile and more adequate to describe different fading situations. The multi-path intensity Nakagami fading pdf of ζ is given by

$$f(\zeta) = \left(\frac{m_T}{\Omega_T}\right)^{m_T} \frac{\zeta^{m_T-1}}{\Gamma(m_T)} \exp\left(\frac{-m_T\zeta}{\Omega_T}\right) \tag{4}$$

where $\Omega_T = \sum_{i=0}^{N_R-1} \Omega_o e^{-i\delta}$, $m_T = \sum_{i=0}^{N_R-1} m_i$, and δ is the exponential decay ratio of the multi-path intensity profile (MIP).

Assuming that there are *J* active users in the system, the received signal is given by

$$r(t) = \sum_{j=1}^{J} \sum_{l=0}^{L} \alpha_{j,l}(t) S_j[t - \tau_{j,l}(t)] e^{j\theta_{j,l}(t)} + \eta(t) \tag{5}$$

where $\eta(t)$ is the AWGN with double-side power spectrum density $\eta_0/2$.

3 Channel Capacity Evaluation

3.1 Effect of Channel Estimation

From the analysis results of W-CDMA system, it has been seen that the channel estimation using pilot symbols suffers from multiple-access interference and multi-path fading. In most publications on coherent demodulation, perfect channel estimation is assumed for the purpose of simplification. Therefore, we considered the channel estimation error in the following performance analysis. In order to mitigate multi-path fading effect, a RAKE receiver with pilot symbol aided coherent demodulation and maximum ratio combining (MRC) is employed. The RAKE receiver structure is shown in figure 2(b), where the number of branches is less or equal to the number of resolvable paths. Assuming that the *i*-th path delay $\tau_{1,i}$ can be accurately estimated for the reference user (*j*=1), each path that corresponds to a RAKE branch gives an output component. The outputs of all branches are added together to form the decision statistic.

Assuming that the fading of each path is independent of each other and the output in each branch of the RAKE receiver is independent of each other, the summed output $Z(m) = \sum_{i=0}^{N_R-1} z_i(m)$ is a Gaussian variable with mean and variance given by

$$\begin{aligned} & E\left\{Z(m)\Big|_{\alpha 1,i(mP_N),\, i=0,1,\ldots,N_R-1}\right\} \\ &= E\left\{Z(m)\Big|_{\zeta}\right\} \\ &= \sum_{i=0}^{R_f-1} E\{z_i(m)\} \end{aligned} \tag{6}$$

and

$$\begin{aligned} &\mathrm{var}\left\{Z(m)\Big|_{\alpha 1, i(mP_N),\, i=0,1,\ldots,N_R-1}\right\} \\ &\quad = \mathrm{var}\left\{Z(m)\Big|_{\zeta}\right\} \\ &\quad = \sum_{i=0}^{R_f-1} \mathrm{var}\left\{z_i(m)\right\} \end{aligned} \tag{7}$$

where R_f is the number of RAKE finger.

Therefore, conditioned on the instantaneous multi-path fading amplitude ζ of the reference user, the equivalent signal-to-noise plus interference ratio (SNIR) is expressed as

$$\gamma_{eq1} = \left\{ \begin{aligned} &\frac{(1+g)}{\zeta}\left(1+\frac{1}{gN_P}\right)\left(\frac{1}{E_b/N_o}+\frac{\Delta\Omega_T J}{2P_N}\right) \\ &+\left(\frac{2N_R(1+g)^2}{\zeta^2 gN_P}\right)\left(\frac{1}{E_b/N_o}+\frac{\Delta\Omega_T J}{2P_N}\right)^2 \end{aligned} \right\}^{-0.5} \tag{8}$$

where $\Delta = 2/3$ for rectangular pulse shaping filter, Ω_T is channel parameter given by $\Omega_T = \sum_{l=0}^{L-1} E\left\{\alpha_{j,l}^2(mN)\right\}$, and E_b/N_o is the signal-to-noise ratio.

3.2 Effect of Multiple-Access Near/Far Interference

As well known, DS/CDMA system is susceptible to multiple-access near/far interference, which occurs when the base station input include one or more other CDMA signals that are stronger by adjusting the transmitted power of mobile users so that the base station gets the same power from the received signal of each transmission. In this paper, we consider the effects of multiple-access near/far interference on performance of the wideband CDMA system with complex spreading scheme that has the channel estimation error. Modifying the previous equation (8), the equivalent SNIR include multiple-access near/far interference is expressed as

$$\gamma_{eq2} = \left\{ \begin{aligned} &\frac{(1+g)}{\zeta}\left(1+\frac{1}{gN_P}\right)\left(\frac{1}{E_b/N_o}+\frac{\Delta\Omega_T}{2P_N}\sum_{j=1}^{J}\frac{P_j}{P_o}\right) \\ &+\left(\frac{2M(1+g)^2}{\zeta^2 gN_P}\right)\left(\frac{1}{E_b/N_o}+\frac{\Delta\Omega_T}{2P_N}\sum_{j=1}^{J}\frac{P_j}{P_o}\right)^2 \end{aligned} \right\}^{-0.5} \tag{9}$$

where P_o is the power controlled reference power.

3.3 Channel Capacity of MIMO CDMA System

Consider a CDMA system with M transmitting antennas and M receiving antennas operating in scattering and path-correlated Nakagami fading channel with different

power profile. Assuming that the transmitted signal is comprised of M statistically independent, equal power components, the expression for channel capacity in bps/Hz is given as [7], [8]

$$C_{M\times M}(\gamma) = \log_2 det\left(\overline{I_M} + \frac{\gamma}{M}\overline{H}\overline{H}^*\right) \tag{10}$$

where det denotes determinant of a matrix, $\overline{I_M}$ is the identity matrix of dimension M where M is the number of transmitting and receiving elements. The superscript * denotes conjugate transpose. Due to the random nature of the $M\times M$ matrix channel transfer function $\overline{H}$, the channel capacity $C_{M\times M}$ is also a random quantity. In the case of $M\times M$ parallel transmission of each path, and the correlation coefficient between any two received paths is ρ, the channel capacity of MIMO wideband CDMA system is obtained as

$$C_{M\times M}(\gamma_{eq}, \rho) = M\log_2\left(1+\frac{\gamma(1-\rho)}{M}\right)+\log_2\left(1+\frac{\rho M\gamma}{M+\gamma(1-\rho)}\right) \tag{11}$$

The received signal is corrupted by AWGN and multiple-access interference signal with statistically independent components of power σ_n^2 and σ_i^2, respectively. The quantity γ_{eq} is independent of M and is a random variable due to Nakagami fading channel. The average channel capacity of MIMO wideband CDMA system, $\overline{C_{M\times M}(\rho,\gamma)}$ is simply the expected value of $C_{M\times M}(\rho,\gamma)$ and is given by

$$\begin{aligned}\overline{C_{M\times M}(\rho,\gamma)} &= \int_0^\infty\cdots\int_0^\infty C_{M\times M}(\rho,\gamma_i)\times\frac{m_f^{m_f}\gamma_i^{m_f}}{\Gamma(m_f)\gamma^{m_f}}\exp\left(\frac{-m\gamma_i}{\gamma}\right)d\gamma_i \\ &= \frac{M\,m_f^{m_f}}{\Gamma(m_f)\,\gamma^{m_f}}\left[\begin{array}{l}\int_0^\infty\cdots\int_0^\infty \log_2\left(1+\frac{\gamma_i(1-\rho)}{M}\right)\times\gamma_i^{m_f}\exp\left(\frac{-m\gamma_i}{\gamma}\right)d\gamma_i \\ +\frac{1}{M}\int_0^\infty\cdots\int_0^\infty \log_2\left(1+\frac{\rho M\gamma_i}{M+\gamma_i(1-\rho)}\right)\times\gamma_i^{m_f}\exp\left(\frac{-m\gamma_i}{\gamma}\right)d\gamma_i\end{array}\right]\end{aligned} \tag{12}$$

where γ_i is the instantaneous SNR and m_f is the Nakagami fading parameter. In order to simplify the numerical evaluation, it is assumed that each user has independent but the same fading characteristics. In general, the integral of equation (12) can be computed numerically using computer software. When the parameters set as $K=1$, $M=1$, $M_C=1$, $m_f=1$, and $\rho=0$, equation (12) reduces to the well-known Shannon capacity formula in Rayleigh fading channel [9].

4 Numerical Results and Discussion

In this section, the effects of different parameters on the channel capacity of wideband CDMA system with complex spreading, imperfect channel estimation by dedicated pilot symbols, and multiple-access near/far interference are investigated by numerical calculations. The multi-path fading is assumed to be Nakagami distributed, and the

exponential decay ratio of MIP model is considered. Unless noted otherwise, the decay ratio of MIP is 0.2, the number of multi-path is 8, the LPF length is 32, and the power ratio of in-phase and quadrature branches is 0.3.

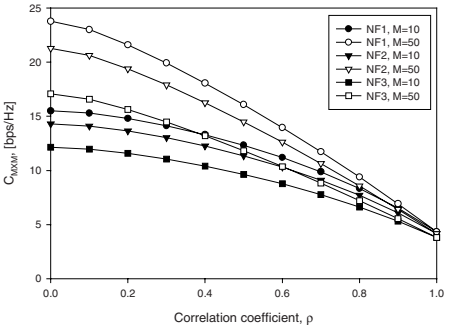

Fig. 3. Channel capacity of MIMO W-CDMA system according to multiple-access interference model and number of MIMO antennas (multiple-access user is 10).

Figure 3 shows the channel capacity of W-CDMA system with imperfect channel estimation as a function of correlation coefficient ρ for different number of antennas, i.e., $M = 10, 50$. Bit-energy-to-noise power density, the number of RAKE fingers, and the number of multiple-access users are set to 15 dB, 8, and 10, respectively. It can be seen that the MIMO scheme takes advantage of the multi-path fading and multiple-access user interference channel and gives better performance as the number of MIMO antennas increases. Also, Fig. 3 illustrates the channel capacity according to the multiple-access near/far interference model and path correlation. In this figure, we select the three kinds of near/far interference model, and NF 1 model show the perfect power control case. According to Fig. 3, NF2 model gives better performance than NF 3 model. This is because NF 2 model has a small variation of power control error than NF 3 model. In order to simplify the performance analysis, we assumed that multiple-access near/far interference model has discrete power and users distribution.

Figure 4 shows the effects of multiple-access near/far interference model and MIMO antennas according to the correlation coefficient ρ when the number of multiple-access users is set to 30. As expected, it is shown that as the number of multiple-access users increase, the channel capacity of MIMO W-CDMA system decrease, and the difference of channel capacity are small according to the multiple-access near/far interference model.

Figure 5 shows the channel capacity of MIMO W-CDMA system with perfect power control according to the parameters N_R and E_b/N_o in multi-path Nakagami fading and multiple-access near/far interference model. The number of Tx/Rx antennas, number of multiple-access user, and path correlation coefficient are set to 10, 10, and 0.4, respectively. In the range of $E_b/N_o \rangle 20\,dB$, the capacity increase for four curves is little. Specially, the difference of channel capacity is same according to the RAKE finger at any E_b/N_o.

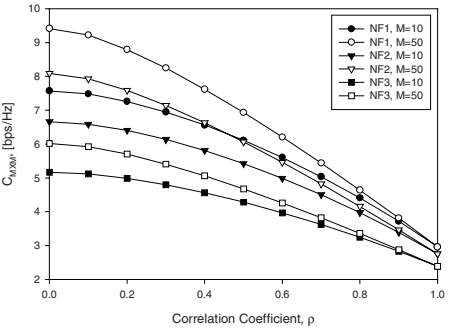

Fig. 4. Channel capacity of MIMO W-CDMA system according to multiple-access interference model and number of MIMO antennas (multiple-access user is 30).

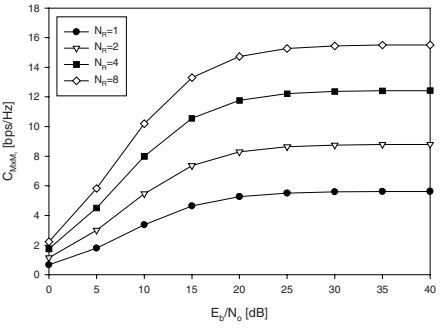

Fig. 5. Channel capacity of MIMO W-CDMA system according to the number of RAKE finger and E_b/N_o at perfect power control case.

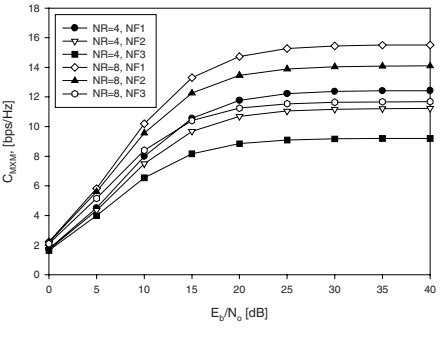

Fig. 6. Channel capacity of MIMO W-CDMA system according to multiple-access interference model, the number of RAKE finger, and E_b/N_o.

Figure 6 shows the channel capacity of MIMO W-CDMA system according to the number of RAKE finger and multiple-access near/far interference model. The number of Tx/Rx antennas, number of multiple-access user, and path correlation coefficient are set to 10, 10, and 0.4, respectively. For small E_b/N_o, the channel capacity increases linearly with E_b/N_o in the range of $E_b/N_o \langle 10\,dB$. But, in the range of $E_b/N_o \rangle 20\,dB$, the channel capacity increases according to the multiple-access near/far interference model.

5 Conclusion

In this paper, the channel capacity of MIMO wideband CDMA system with imperfect channel estimation and multiple-access near/far interference in path-correlated Nakagami fading channel is evaluated. The following conclusions have been drawn. The effects of multi-path fading, imperfect channel estimation error, and multiple-access interference can be suppressed by RAKE receiver, I/Q complex spreading and multiple Tx/Rx antennas scheme. The system capacity degrades significantly due to the multiple-access near/far interference. However, this interference can be effectively limited by power control and channel estimation scheme. Employing the multi-element arrays at both transmitter and receiver can lead to increase the spectral efficiency for a given total transmit power in a scattering channel. From the results, the MIMO wideband CDMA with RAKE receiver scheme improves the equivalent SNIR from the multiple-access users in MIMO wireless channel. The channel capacity of the proposed MIMO wideband CDMA system may be as high as 4~5 times that with the conventional SISO system for the case of $M = 10$ and $0 \langle \rho \langle 0.4$.

Acknowledgements. This work was supported by the Korea Science & Engineering Foundation (KOSEF) and the Kyonggi Province through the Internet Information Retrieval Research Center (IRC) of Hankuk Aviation University.

References

1. J. Wang and J. Chen, “Performance of wideband CDMA systems with complex spreading and imperfect channel estimation,” IEEE J. Select. Areas Commun., vol. 19, no. 1, pp. 152–163, Jan. 2001.
2. F. Adachi, M. Sawahashi, and H. Suda, “Wideband DS-CDMA for next generation mobile communications systems,” IEEE Commun. Mag., vol. 36, pp. 56–69, Sept. 1998.
3. 3G TS 25.213 version 3.3.0, “Spreading and modulation (FDD),” 3GPP TSG-RAN, 2000-06.
4. L. Staphorst, M. Jamil, and L. P. Linde, “Performance evaluation of a QPSK system employing complex spreading sequences in a fading environment,” in Proc. IEEE VTS 50th Vehicular Technology Conf., pp. 2964–2968, Sept. 1999.
5. T. G. Macdonald and M. B. Pursley, “Complex processing in quaternary direct-sequence spread-spectrum receivers,” in Proc. IEEE Military Communications Conf., pp. 494–498, Oct. 1998.

6. T. Eng and L. B. Milstein, "Coherent processing in quaternary direct-sequence spread-spectrum receivers," IEEE Trans. Commun., vol. 43, pp. 1134–1143, Feb./Mar./Apr. 1995.
7. G. J. Foschini, "Layered space-time architecture for wireless communication in a fading environment when using multiple antennas," Bell Labs Tech. J., pp. 41–59, Autumn, 1996.
8. S. L. Loyka and J. Mosig, "Channel capacity of n-antenna BLAST architecture," Electr. Lett., vol. 36(7), pp. 660–661, March 2000.
9. W. C. Y. Lee, "Estimate of channel capacity in Rayleigh fading environment," Trans. on Veh. Technol., vol. 39, no. 3, Aug. 1990.